SURE 静岡大学学術リポジトリ
Shizuoka University REpository

Synthesis of a self-assembling gold nanoparticle-supported organocatalyst for enamine-based asymmetric aldol reactions

メタデータ	言語: English 出版者: 公開日: 2018-03-14 キーワード (Ja): キーワード (En): Organocatalyst, Supported catalysis, Nanoparticle, Aldol reaction 作成者: Sóti, Péter Lajos, Yamashita, Hiroki, Sato, Kohei, Narumi, Tetsuo, Toda, Mitsuo, Watanabe, Naoharu, Marosi, György, Mase, Nobuyuki☒ メールアドレス: 所属:
URL	http://hdl.handle.net/10297/00024833

■ **Graphical Abstract**

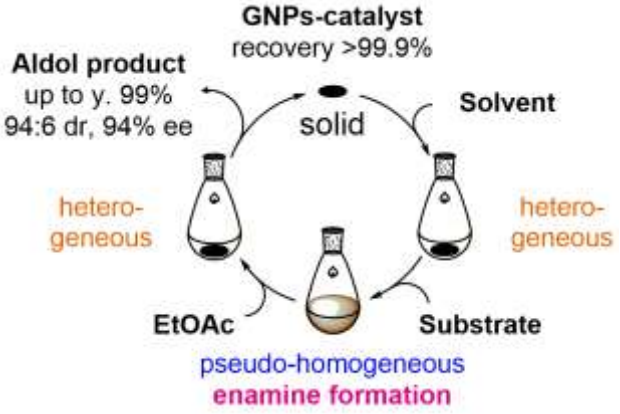

■ **Title**

Synthesis of a self-assembling gold nanoparticle-supported organocatalyst for enamine-based asymmetric aldol reactions

■ **Authors**

Péter Lajos Sóti[a,b], Hiroki Yamashita[b], Kohei Sato[b], Tetsuo Narumi[b,c], Mitsuo Toda[b], Naoharu Watanabe[b,c], György Marosi[a] and Nobuyuki Mase[b,c,d,*]

■ **Affiliations**

[a] Department of Organic Chemistry and Technology, Budapest University of Technology and Economics, Budafoki ut 8, Budapest, H-1111, Hungary

[b] Applied Chemistry and Biochemical Engineering Course, Department of Engineering, Graduate School of Integrated Science and Technology, Shizuoka University, 3-5-1 Johoku, Hamamatsu, Shizuoka 432-8561, Japan

[c] Graduate School of Science and Technology, Shizuoka University, 432-8561, Japan

[d] Green Energy Research Division, Research Institute of Green Science and Technology, Shizuoka University, 432-8561, Japan

■ **Corresponding author**

Tel.: +81-53-478-1196; fax: +81-53-478-1196; e-mail: mase.nobuyuki@shizuoka.ac.jp

■ **Abstract**

The self-assembling gold nanoparticle (GNP)-supported L-proline derivative, which was readily synthesized in four steps from 4-hydroxy-L-proline and chloroauric acid, was used for enamine-based aldol reactions. The modified Brust-Schiffrin (BS) synthesis was favored over

the ligand exchange reaction in order to develop a new and simple synthetic pathway for nanoparticle-supported catalyst. Use of immobilized organocatalyst on nanoscale solid carrier led to excellent selectivities (up to 94:6 dr and 94% ee) in asymmetric reactions of ketones and benzaldehydes. GNPs operate under pseudo-homogeneous conditions which are easily recycled and reused at least five times without significant loss of weight, activity, diastereo- and enantioselectivities.

■ Keywords

Organocatalyst, Supported catalysis, Nanoparticle, Aldol reaction

■ Introduction

Organocatalysts are widely applied for asymmetric reactions in organic synthesis.[1,2] Proline and proline-based derivatives represent organocatalysts that show high catalytic activity and stereoselectivity in asymmetric C–C bond forming reactions such as the aldol,[3] Mannich,[4] Michael,[5] and Diels-Alder reactions[6] via enamine and iminium intermediates.[7] Unfortunately, high catalyst loadings (up to 30 mol%) are required in many cases;[3-7] therefore, recycling and reuse of the active catalyst is required to ensure the environment-friendly character of these catalytic processes. In general, problems related to catalyst recycling and reuse can be solved by immobilization on a solid carrier[8-10] and impressive progress has been made over recent years in this area;[11-13] however, the catalytic reaction becomes heterogeneous and loses the benefits of homogeneous phase conditions.[14] If the catalyst is immobilized on a nanoscale solid carrier, the benefits of both heterogeneous and homogeneous catalytic reactions can be combined (Figure 1).[15,16]

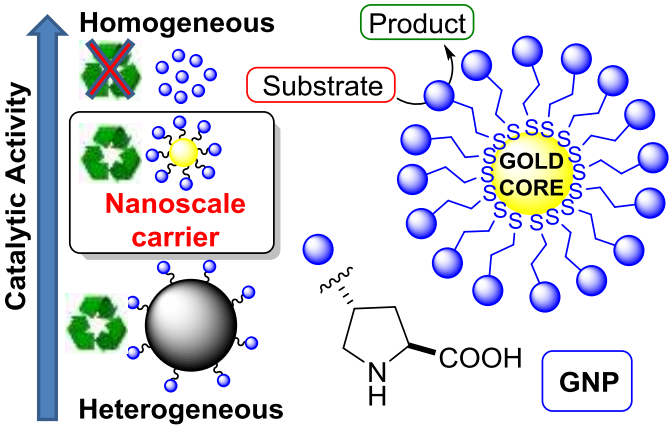

Figure 1. GNP-supported L-proline derivatives as organocatalysts

Recently, magnetic nanoparticle-supported organocatalysts were reported; however, the use of a magnetic nanocore as a carrier requires several synthetic steps to immobilize the catalyst.[17-20] Thus, our attention turned to the Brust-Schiffrin (BS) synthesis, a well-known bottom-up method to prepare ligand-protected metal core nanoparticles.[21-24] This method allows the formation of metal nanocore and complete capping of metal nanocores with a catalytically active component in a single synthetic step. Very recently, Santacruz *et al.* reported the preparation and application of a gold nanoparticle (GNP)-supported cinchonine derivative.[25] This supported catalyst showed moderate selectivity during recycling similar to an earlier study by Malkov *et al.*,[26] which was explained by the loss of the catalyst from the support. Khiar *et al.* also reported the preparation and application of GNP-supported organocatalyst though the yield of aldol product dropped significantly to 30% after the third recycling run.[27] To the best of our knowledge, there is no report on complete capping of metal nanocores with a organocatalytically active component in a single synthetic step. Therefore, we aimed to synthesize a GNP-supported organocatalyst by a modified one-phase BS method (single synthetic step) instead of ligand exchange to overcome the mentioned disadvantages of nanoparticles supported catalyst.

■ Results and Discussion

Using the one-phase BS method, Au(III) ions are first reduced to Au(I) by thiols, which leads to the formation of $[Au(I)\text{-}SR]_n$.[28] To avoid the formation of undesired metal thiolate polymer that cannot be reduced completely to the thiolate monolayer-protected gold core by sodium borohydride,[29] disulfide derivate **3** was used as the self-assembling component instead of the thiol. Therefore, the first step for the preparation of GNPs was protection of the thiol functional group by oxidation,[30] which led to the formation of a disulfide bond between two molecules of thiol **1** (Scheme 1). The resulting bifunctional carboxylic acid **2** was converted to 11,11'-disulfanediyldiundecanoyl chloride with oxalyl chloride, and subsequently used for chemoselective *O*-acylation of 4-hydroxy-L-proline (**5**) in an acidic medium without isolation to prevent unwanted *N*-acylation.[31]

With key intermediate **3** in hand, we studied the self-assembly of the GNP-supported catalyst; the results are summarized in Table 1. The catalyst loading of the final product strongly depended on the modified BS synthesis conditions. We found that the amount of immobilized catalyst could be improved from 0.50 to 0.95 mmol g^{-1} by increasing the addition time of sodium borohydride.

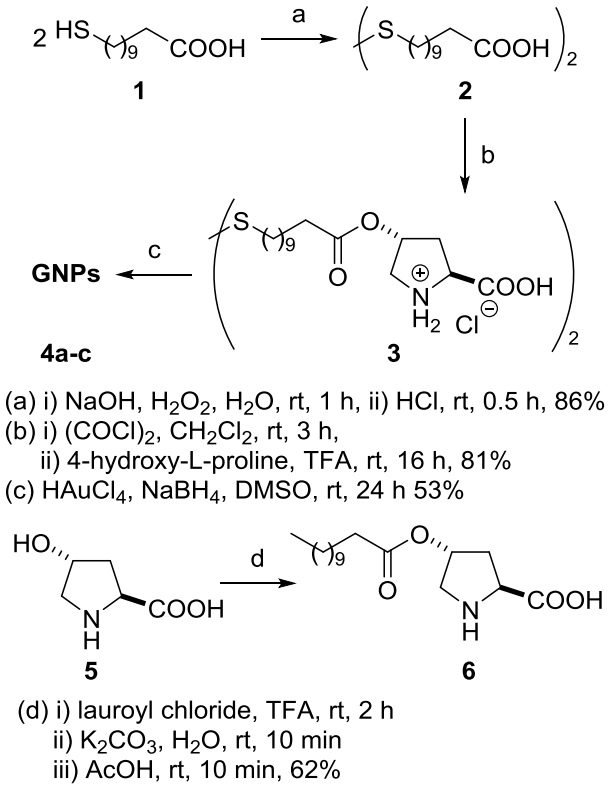

Scheme 1. Synthesis of GNP-supported and *O*-lauroyl-*trans*-4-hydroxy-L-proline catalysts

Table 1. Self-assembly of GNP-supported organocatalysts

entry	catalyst	$NaBH_4$	addition time (min)	catalyst loading (mmol g^{-1})[a]	particle size (nm)[b]
1	**4a**	solid	<1	0.50	-
2	**4b**	solution	30	0.71	~3
3	**4c**	solution	60	0.95	~3

[a] Determined by elemental analysis based on the nitrogen atom wt% (nitrogen as an indicator atom for the proline moiety on the Au core). [b] Determined based on TEM analysis.

Transmission electron microscopy (TEM) showed that the particles have a spherical shape with a diameter of about 3 nm, and their physical properties are independent of the preparation process (Figure 2). Aggregation of the particles was observed in the case of **4b** with a lower catalyst loading (Figure 2, left image). Moreover, **4a** could not be dispersed in the DMSO/cyclohexanone medium used to prepare the colloids for TEM investigations. The dispersion of **4c** showed randomly distributed and well-dispersed single particles without any aggregates (see figure 2 right image and the supporting information).

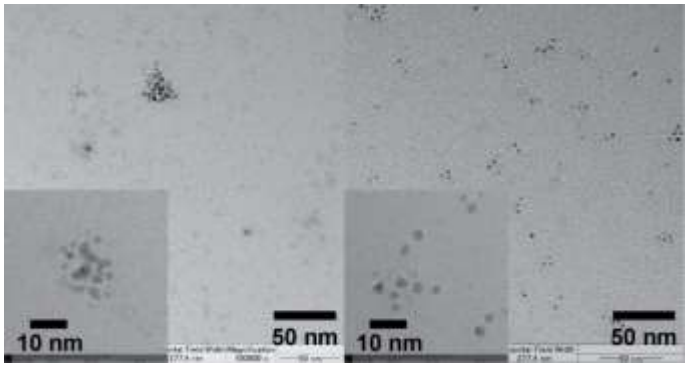

Figure 2. TEM Images of GNPs **4b** (left) and **4c** (right)

The colloidal properties of ligand-protected Au clusters were examined by UV/VIS spectroscopy to gain further information about the properties of **4b** and **4c**.[32] A surface plasmon (SP) band appeared at 512 nm in **4c**, with the highest catalyst loading, in contrast to **4b**, where an SP band was undetectable (Figure 3). This result is consistent with our prior assumption, *i.e.*, the proline content promotes the dispersion of the supported catalyst in a medium.

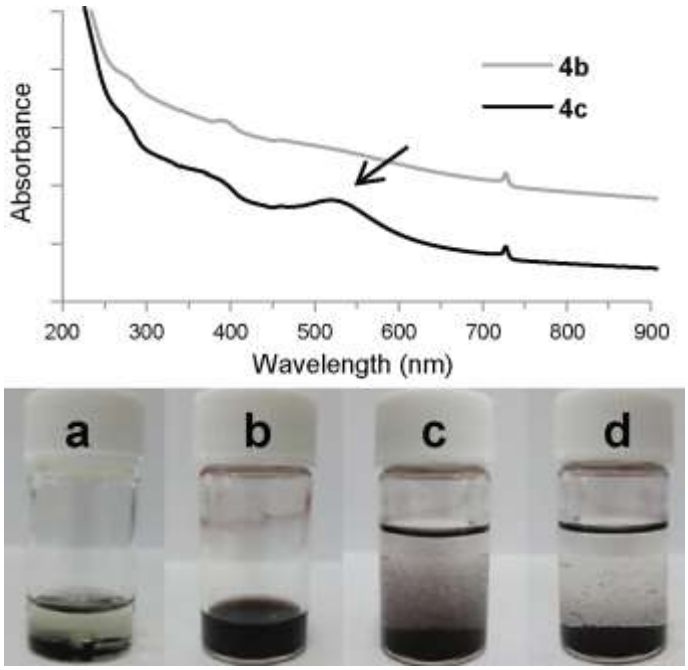

Figure 3. Colloidal behavior of supported catalyst: UV/VIS spectra of **4b** and **4c**; Images of reaction mixtures: (a) at 0 h, (b) after 24 h, (c) after addition of EtOAc and (d) following 2 min of storage.

IR spectrometry was used to confirm the chemical structure of the supported catalyst. According to the IR spectra, the functional group peaks of the GNPs **4c** correspond to *O*-

lauroyl-*trans*-4-hydroxy-L-proline (native catalyst, **6**),[33] where typical bands for the free amine (1611 cm^{-1}), carbonyl (1732 cm^{-1}), and alkyl groups (2850 and 2917 cm^{-1}) were observed (Figure 4).

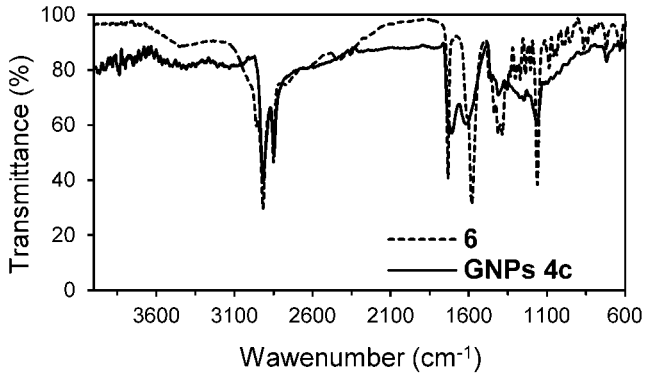

Figure 4. IR spectra of **4c** and **6**

To demonstrate the catalytic activity of the GNP-supported catalyst, **4c** was investigated in asymmetric aldol reactions (Table 2). GNP **4c** was easily and finely dispersed in the reaction mixture (Figure 3-b), and showed high activity. In most cases, the reactions afforded the *anti*-aldol products in high yields with high to excellent diastereo- and enantioselectivities (Table 2). Compounds **9a-h** were obtained with good results up to 99% yield and 89% ee. As shown in Table 2, the substituents on the benzaldehyde can greatly influence the reactivities. A comparison of entries 1 and 7 indicates that the reaction time can be reduced by electron-withdrawing groups, with an associated increase in enantioselectivity from 77% to 88% ee. Using *p*-methoxy benzaldehyde as an acceptor, the immobilized organocatalyst afforded aldol product **9f** with 85:15 dr and 78% ee. Therefore, the supported catalyst tolerates both electron-withdrawing and electron-donating substituents in the direct asymmetric aldol reaction, which is consistent with the unsupported catalyst.[3]

Table 2. GNP-supported proline-catalyzed asymmetric aldol reactions.

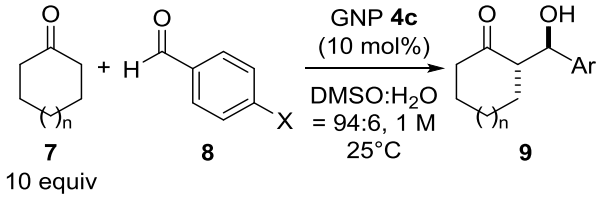

entry	n	X	time (h)	yield (%)[a]	dr[b]	ee (%)[c]	product
1	1	NO_2	24	97	90:10	88	**9a**
2	1	Cl	72	99	91:9	89	**9b**
3	1	Br	72	90	90:10	87	**9c**
4	1	CN	48	99	90:10	83	**9d**
5	1	CO_2Me	72	99	90:10	86	**9e**
6	1	OMe	166	23[e]	85:15	78	**9f**
7	1	H	120	65	91:9	77	**9g**
8	0	NO_2	5	98	35:65	78	**9h**

[a] Isolated yield. [b] Determined by ^{1}H-NMR (*anti*:*syn*). [c] Enantiomeric excesses of the *anti*-products were determined by chiral HPLC analysis. [e] Conversion of the aldehyde was 31% based on ^{1}H-NMR.

The recyclability of the supported catalyst was examined for 1-5 cycles in the direct aldol reaction between **7a** and **8a** (Table 3). After 24 h, a fine dispersion of nanoparticles was obtained (Figure 3-b), and the GNPs were recovered by changing the dielectric constant of the reaction mixture by the addition of EtOAc. Based on the colloidal behavior, the GNPs aggregated immediately (Figure 3-c) and the reaction mixtures became heterogeneous, thus facilitating the separation of immobilized organocatalyst and aldol product. The nanoparticles could be recovered by decantation after centrifugation. Consequently, while **4c** has the physical properties of a heterogeneous catalyst, during the enamine cycle it operates in a pseudo-homogenous phase due to the formation of more soluble enamine intermediates on the gold core in organic solvents (see graphical abstract).

As shown in Table 3, the reaction times, yields, conversions, and stereoselectivities were unchanged during the recycling process, which indicates the high efficiency of our supported catalyst **4c**. The unchanged reaction times (exactly 24 h) point out the unchanged catalytic activities which presumably rule out the possibility of any aggregation of nanoparticles in the reaction mixture.

The recovery of the GNP **4c** was determined by weight measurement and residual metal content of the reaction mixture. According to inductively coupled plasma optical emission spectroscopy (ICP-OES) measurements, the residual gold was less than 2 µg (<0.03%) (See supporting information).

Table 3. Recycling of GNP-supported proline catalyst **4c**

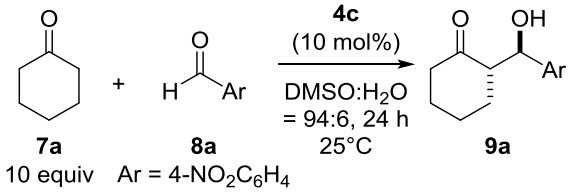

cycles	conversion (%)[a]	yield (%)[b]	dr[c]	ee (%)[d]	recovery (%)
1	98	97	90:10	88	≥99
2	99	98	91:9	88	≥99
3	99	98	91:9	88	≥99
4	99	98	92:8	88	≥99
5	99	98	92:8	88	≥99

[a] Determined by ^{1}H-NMR. [b] Isolated yield. [c] Determined by ^{1}H-NMR (*anti*:*syn*). [d] Enantiomeric excesses of the *anti*-products were determined by chiral HPLC analysis.

To investigate the stereoselectivity of the supported-catalyst, we compared it with native catalyst **5** (4-hydroxyl-L-proline) and **6** (*O*-lauroyl-*trans*-4-hydroxy-L-proline), in the direct aldol reaction between **7a** and **8a** (Table 4). In the case of catalysts **5** and **6**, the enantioselectivities were 94% and 95%, respectively (entries 1 and 2). With supported catalyst **4c**, increasing the loading to 20 mol% improved the dr and ee of aldol product **9a** from 90:10 to 94:6 and from 88% to 94%, respectively, when the reactions were performed at 0 °C (entries 4 and 5). Based on these results, similar stereoselectivities can be achieved by varying the reaction conditions of the immobilized catalyst **4c**. On the other hand, GNP-supported catalyst **4b** with less catalyst loading showed lower diastereo- and enantioselectivities (entry 4).

We then compared the reactivities of immobilized **4c** and unsupported catalysts (**5**, **6**) in the aldol reaction progress of **7a** and **8a**. Conversions were determined by monitoring the reaction mixtures by ^{1}H NMR. The conversion vs. reaction time diagram shows similar reaction progress (at 12 h ~30% conversion), although the catalytic activity of **4c** is slightly lower than that of **5** and **6** after 12 h (Figure 5).

Next, the substrate concentrations of aldol reaction were decreased from 1 M to 0.05 M in order to investigate its effect for the asymmetric induction (Table 4, entries 6-8). Surprisingly, the enantioselectivities of catalysts **5** and **6** were lower (74% and 76% ee, respectively) than that of the GNP (89% ee) at 0.05M, namely the stereoselectivities are influenced by the substrate concentration in the case of the unsupported catalysts (Table 4, entry 1, 2, 6, and 7), but the stereoselectivities of the immobilized catalyst **4c** were unchanged (Table 4, entry 4 and 8).

Table 4. Comparison of unsupported catalysts (**5** and **6**) and GNP catalyst in the aldol reaction

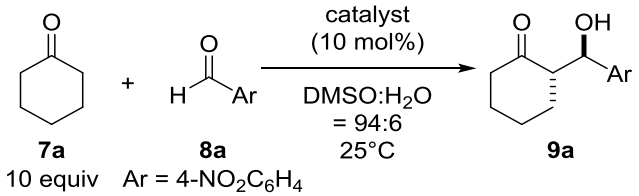

entry	catalyst	concentration (M)	time (h)	yield (%)[a]	dr[b]	ee (%)[c]
1	**5**	1	16	97	86:14	94
2	**6**	1	16	98	92:8	95
3	**4b**	1	24	98	83:17	73
4	**4c**	1	24	97	90:10	88
5[d]	**4c**	1	40	97	94:6	94
6	**5**	0.05	72	97	95:5	74
7	**6**	0.05	72	98	97:3	76
8	**4c**	0.05	90	98	92:8	89

[a] Isolated yield. [b] Determined by ^{1}H-NMR (*anti*:*syn*). [c] Enantiomeric excesses of the *anti*-products were determined by chiral HPLC analysis. [d] The reaction was carried out at 0 °C with 20 mol% catalyst.

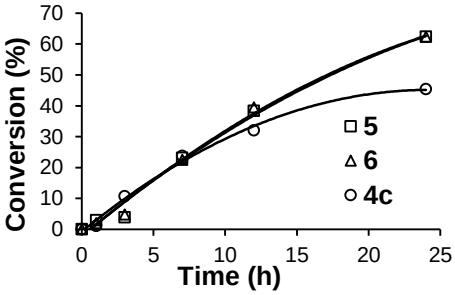

Figure 5. Comparison of unsupported catalysts (**5** and **6**) and GNP catalyst (**4c**) in the aldol reaction (See the reaction conditions in the Table 4 entry 6, 7, and 8).

These results could be explained by the neighbor interactions of nearby catalyst moieties on the nanoscale carrier. Considering the one-proline-mechanism of proline-catalyzed aldolization,[34] it is due to the neighboring long alkyl chain of catalyst species which could provide "reactive environment"[35,36] for the substrates and for the intermediates on the gold nanocore hence the molecular environment of substrates does not change by dilution. While in the case of unsupported catalysts, the molecular environment of intermediates and catalyst molecules changed by dilution resulting decreased enantioselectivities.

Our "reactive environment" is also supported by the results of **4b** (0.71 mmol g^{-1} catalyst loading of GNP) catalyzed aldol reaction. As shown in Table 4 (entry 3 and 4), decreasing the number of catalyst species from 0.95 to 0.71 mmol g^{-1} on the gold nanocore (in other words: change the reactive environment and size of reactive pocket) led to lower enantioselectivity (from 88% to 73% ee). This effect is similar to the catalytic mechanism of enzymatic transformations in the biological systems *i.e.* our GNP can be interpreted as an artificial enzyme where one of the catalytically active molecules on the surface of nanocore seems to be an active center of the enzyme (see Figure 1).

■ Conclusion

Proline-functioned GNPs were synthesized and applied in the asymmetric aldol reaction of benzaldehyde derivatives and cyclic donors, resulting in aldol products with high to excellent stereoselectivities. The recycling efficiency of our nanoparticle-supported catalyst was excellent, without significant loss of weight, activity, and selectivity. These results pointed out that the preparation processes strongly influence it. In addition, the supported catalyst's activity is comparable with that of the native counterparts, and the enantioselectivity of the immobilized catalyst is independent on the substrate concentration due to the unchanged molecular environment of substrates. Although the gold as a carrier material is slightly

expensive; the preparation of GNP-supported proline required only four easy and simple synthetic steps while magnetic nanoparticle- or polymer-supported organocatalysts require many synthetic steps and longer synthetic process which tend to raise their cost. Furthermore, the recycling study showed that the recovery of GNPs is excellent and not required any special processes. Considering all these advantages of GNPs, our new synthetic pathway for the immobilization of catalyst can promote an alternative route in the field of supported catalysis.

■ Experimental

Synthesis of GNP-supported catalyst

11,11'-Dithiobis(undecanoic acid) (2).[30,37] To a suspension of 11-mercaptoundecanoic acid (1.15 g, 5.00 mmol) in H_2O (540 mL) was added sodium hydroxide (2.80 g, 67.9 mmol) and hydrogen peroxide solution (30 wt%, 11 mL) was filled to a well-stirred clear solution. After being stirred for 90 min, concentrated HCl (37 wt%, 11 mL) was added and the mixture was extracted with EtOAc (3×150 mL). The organic solution was washed with distilled water (2×50 mL), saturated aqueous NaCl (50 mL) and dried over Na_2SO_4. After removing the solvent, disulfide **2** was obtained as a white solid (945 mg, 87%). mp 90.8 - 92.2 °C; ^{1}H NMR (300 MHz, DMSO-d6) δ 1.18-1.34 (m, 24H), 1.43-1.52 (m, 4H), 1.54-1.66 (m, 4H), 2.18 (t, J = 7.3 Hz, 4H), 2.69 (t, J = 7.2 Hz, 4H); ^{13}C NMR (75 MHz, DMSO-d6) δ 24.5, 27.8, 28.6, 28.6, 28.8, 28.9, 29.9, 33.7, 38.0, 174.6.

(2*S*,2'*S*,4*R*,4'*R*)-4,4'-((11,11'-Disulfanediylbis(undecanoyl))bis(oxy))bis(2-carboxypyrrolidin-1-ium) chloride (3). The disulfide **2** (300 mg, 0.69 mmol) was suspended in dichloromethane (3.1 mL) in argon atmosphere and oxalyl chloride (0.2 mL, 2.44 mmol) was dropped to a well-stirred reaction mixture at room temperature. A resulted peal yellow but clear solution was evaporated by vacuum pump after 3 h reaction time, keeping in argon atmosphere. Previously recrystallized *trans*-4-hydroxy-L-proline (181 mg, 1.38 mmol) was dissolved in TFA (3.1 mL) by stirring at room temperature in argon atmosphere. The solution was cooled just below room temperature with an ice/water bath and it was added by a syringe in one portion for acid chloride. The reaction mixture was stirred at room temperature for 24 h. Under cooling with an ice/water bath, Et_2O (20 mL) was added carefully to give a russet sticky solid which was decanted, washed with Et_2O (3×10 mL) and dried in vacuum for 48 h to give proline derivative **3** as a russet solid (372 mg, 73%). mp 74.4-77.7 °C (dec.); $[\alpha]^{19}_D$ -10.2 (c 0.1, MeOH); IR (neat, cm^{-1}): 720, 1154, 1210, 1745, 2850, 2917; ^{1}H NMR (300 MHz,

CD_3OD) δ 1.26-1.41 (m, 24H), 1.57-1.73 (m, 8H), 2.34-2.48 (m, 6H), 2.53-2.64 (m, 2H), 2.68 (t, J = 7.5 Hz, 4H), 3.42-3.55 (m, 2H), 3.68 (dd, J = 13.5, 4.5 Hz, 2H), 4.57 (dd, J = 10.5, 7.5 Hz, 2H), 5.39-5.49 (m, 2H); ^{13}C NMR (75 MHz, DMSO-d6) δ 24.1, 27.7, 28.4, 28.5, 28.6, 28.7, 28.8, 28.9, 33.4, 34.2, 37.9, 50.2, 53.1, 57.7, 68.6, 72.1, 169.6, 170.4, 172.6, 174.6; HRMS (ESI, m/z): calcld for $C_{32}H_{56}N_2O_8S_2$ ($M+H^+$) 661.35563, found 661.35649.

Preparation of GNP supported catalyst 4c. A 500 mL eggplant-shaped flask, which was flushed argon gas previously, was charged with gold(III) chloride·$4H_2O$ (338 mg, 0.82 mmol), disulfide derivative of proline **3** (300 mg, 0.41 mmol) and dehydrated DMSO (410 mL) was added, keeping in argon atmosphere. To the clear bright yellow solution, sodium borohydride solution (169 mg, 4.10 mmol in MeOH (14.4 mL)) was dropped over 1 h and the resulted black suspension was stirred at room temperature for 24 h. During the working up, the black solid component was decanted, washed with EtOH (2×15 mL), AcOH (2×10 mL), EtOH (6×15 mL), Et_2O (1×15 mL), respectively, and dried in vacuum at room temperature to give GNP supported catalyst **4c** as a black solid (228 mg, 53%). Elemental analysis: C: 20.81%, H: 2.84%, N: 1.33%, S: 3.71%; IR (neat, cm^{-1}): 633, 1163, 1410, 1617, 1709, 2847, 2917.
Above mentioned process was used for preparation of **4a** (yield: 206 mg, 48%) and **4b** (yield: 210 mg, 49%) but in case of **4a**, solid sodium borohydride was added to the reaction mixture in one portion and in case of **4b**, the dropping time of sodium borohydride solution was 30 min.
Elemental analysis (**4a**): C: 10.43%, H: 1.42%, N: 0.70%, S: 1.95%;
Elemental analysis (**4b**): C: 20.19%, H: 2.83%, N: 0.99%, S: 4.07%.

Preparation and characterization of *O*-lauroyl-*trans*-4-hydroxy-L-proline (6).[31] *trans*-4-Hydroxy-L-proline (**5**, 500 mg, 3.81 mmol) was dissolved in TFA (2.1 mL) at room temperature in argon atmosphere. To the solution, lauroyl chloride (1.7 mL, 7.63 mmol) was added in one portion and the solution was stirred at room temperature for 2 h. Et_2O (7.5 mL) was added under cooling with an ice/water bath to give a fine white precipitate which was vacuum filtered, washed with Et_2O (5 mL) and dried in vacuum at room temperature. The hydrochloride salt of **6** was dissolved in boiling MeOH (2 mL) and hot MTBE (3 mL) was added to the boiling solution which was left to crystallize for 5h at room temperature. The crystals were vacuum filtered and dried in vacuum at room temperature. The recrystallized hydrochloride salt (100 mg, 0.29 mmol) was dissolved in 10% K_2CO_3 solution (2 mL) stirred for 10 min and AcOH was added to adjust pH to 7. The solid precipitate was filtered and

recrystallized from MeOH (1 mL) to give **6** as white needle shape crystals (56 mg, 62%). mp 185.4-187.4 °C (dec.); $[\alpha]^{19}_{D}$ -17.9 (*c* 0.09, MeOH); IR (neat, cm^{-1}): 633, 718, 1161, 1581, 1612, 1733, 2850, 2917 (see Figure 4); ^{1}H NMR (300 MHz, CF_3COOD) δ 0.76 (t, *J* = 6.5 Hz, 3H), 1.12-1.28 (m, 16H), 1.52-1.69 (m, 2H), 2.42 (t, *J* = 7.7 Hz, 2H), 2.52-2.65 (m, 1H), 2.74-2.88 (m, 1H), 3.81-3.96 (m, 2H) 4.85-4.95 (m, 1H), 5.78-5.60-5.66 (m, 1H); ^{13}C NMR (75 MHz, CF_3COOD) δ 14.7, 24.4, 26.7, 31.0, 31.0, 31.3, 31.3, 31.5, 31.5, 33.9, 36.9, 54.9, 61.6, 75.8, 177.7, 180.5.

General method for aldol reaction using GNP supported proline catalyst

Benzaldehyde derivatives **8** (0.06 mmol), GNPs, aldol donor **7** (10 equiv), DMSO:water (94:6, 65 μL) solvent mixture and magnetic stir bar were added to a 2 mL capped glass vial and it was stirred at 25 or 0°C. Conversion was monitored by TLC. During the working up, the reaction mixture was diluted with EtOAc (1 mL) and the liquid phase was removed by decantation after 2 min of centrifugation at 4000 rpm. The solid residue was suspended in EtOAc (1 mL) and the previous procedure was used for separation of the liquid phase after 10 min of stirring, and this procedure was repeated twice. The combined organic solutions were filtered through a sort silica pad, washed with distilled water (3 mL), dried over Na_2SO_4, and the solvent was evaporated. The diastereomeric ratios of the crude products (**9a-h**) were determined by ^{1}H NMR after evaporation. The enantiomeric excesses of anti-products **9b-h** were determined by chiral HPLC analysis after purification of the crude products by preparative TLC. For preparative TLC, hexane-ethyl acetate solvent mixtures were used as eluent. In the case of **9a**, the crude product was used directly for chiral HPLC analysis. The absolute configuration of aldol products **9** were determined by comparison of the HPLC-data with our previous results.[38]

Recycling of GNPs

General method was used during the recycling. The supported catalyst **4c** was reused after overnight drying in vacuum at room temperature without further treatment.

Characterization of aldol products

(*S*)-2-((*R*)-Hydroxy(4-nitrophenyl)methyl)cyclohexanone (9a).[38] yield: 14.5 mg, 97%; diastereomer ratio 94:6, determined by ^{1}H NMR of crude product. Colorless solid; mp 129-130 °C; $[\alpha]^{19}_{D}$ +6.3 (*c* 0.1, $CHCl_3$); ^{1}H NMR (300 MHz, $CDCl_3$) δ 1.18-1.91 (m, 5H), 1.97-2.23 (m, 1H), 2.25-2.69 (m, 3H), 4.08 (s, 1H), 4.90 (d, *J* = 8.4 Hz, 1H), 7.51 (d, *J* = 8.8 Hz,

2H), 8.22 (d, J = 8.8 Hz, 2H); ^{13}C NMR (75 MHz, $CDCl_3$) δ 24.8, 27.7, 30.8, 42.8, 57.3, 74.2, 123.8, 128.1 148.6, 215.1. Enantiomeric excess of *anti*-product: 94%, determined by HPLC (Daicel Chiralpak IB, Hexane/*i*-PrOH = 90/10), UV λ = 254 nm, flow rate 0.5 mL/min, t_R (2*S*, 1'*R*) 28.5 min, t_R (2*R*, 1'*S*) 33.5 min.

(*S*)-2-((*R*)-(4-Chlorophenyl)(hydroxy)methyl)cyclohexanone (9b).[38] yield: 14.2 mg, 99%; diastereomer ratio 91:9, determined by ^{1}H NMR of crude product. Colorless solid; mp 95-96 °C; $[\alpha]^{19}_D$ +22.5 (*c* 0.1, $CHCl_3$); ^{1}H NMR (300 MHz, $CDCl_3$) δ 1.20-1.80 (m, 5H), 2.00-2.12 (m, 1H), 2.24-2.60 (m, 3H), 3.99 (s, 1H), 4.74 (d, J = 8.7 Hz, 1H), 7.20-7.33 (m, 4H); ^{13}C NMR (75 MHz, $CDCl_3$) δ 24.8, 27.8, 30.8, 42.8, 57.5, 74.3, 128.6, 128.8, 133.8, 139.7, 215.7. Enantiomeric excess of *anti*-product: 89%, determined by HPLC (Daicel Chiralpak AD-H, Hexane/*i*-PrOH = 90/10), UV λ = 254 nm, flow rate 0.5 mL/min, t_R (2*S*, 1'*R*) 27.0 min, t_R (2*R*,1'*S*) 31.3 min.

(*S*)-2-((*R*)-(4-Bromophenyl)(hydroxy)methyl)cyclohexanone (9c).[38] yield: 15.3 mg, 90%; diastereomer ratio 90:10, determined by ^{1}H NMR of crude product. Colorless solid; mp 82-83 °C; $[\alpha]^{19}_D$ +17.1 (*c* 0.1, $CHCl_3$); ^{1}H NMR (300 MHz, $CDCl_3$) δ 1.22-1.77 (m, 5H), 2.03-2.13 (m, 1H), 2.31-2.60 (m, 3H), 3.97 (d, J = 2.7 Hz, 1H), 4.75 (dd, J = 8.7, 2.3 Hz, 1H), 7.20 (d, J = 8.3 Hz, 2H), 7.48 (d, J = 8.3 Hz, 2H); ^{13}C NMR (75 MHz, $CDCl_3$) δ 24.8, 27.8, 30.8, 42.8, 57.4, 74.4, 121.9, 129.0, 131.7, 140.3, 215.6. Enantiomeric excess of *anti*-product: 87%, determined by HPLC (Daicel Chiralpak AD-H, Hexane/*i*-PrOH = 90/10), UV λ = 254 nm, flow rate 0.5 mL/min, t_R (2*S*, 1'*R*) 29.2 min , t_R (2*R*,1'*S*) 34.3 min.

4-((*R*)-Hydroxy((*S*)-2-oxocyclohexyl)methyl)benzonitrile (9d).[38] yield: 13.6 mg, 99%; diastereomer ratio 90:10, determined by ^{1}H NMR of crude product. Colorless solid; mp 82-83 °C; $[\alpha]^{19}_D$ +19.5 (*c* 0.1, $CHCl_3$); ^{1}H NMR (300 MHz, $CDCl_3$) δ 1.18-1.93 (m, 5H), 1.99-2.19 (m, 1H), 2.25-2.69 (m, 3H), 4.04 (s, 1H), 4.84 (d, J = 8.7 Hz, 1H), 7.45 (d, J = 8.1 Hz, 2H), 7.65 (d, J = 8.1 Hz, 2H); ^{13}C NMR (75 MHz, $CDCl_3$) δ 24.8, 27.7, 30.8, 42.8, 57.3, 74.4, 111.9, 118.9, 128.0, 132.4, 146.6, 215.2. Enantiomeric excess of *anti*-product: 86%, determined by HPLC (Daicel Chiralpak AD-H, Hexane/*i*-PrOH = 90/10), UV λ = 254 nm, flow rate 0.5 mL/min, t_R (2*S*, 1'*R*) 46.7 min, t_R (2*R*,1'*S*) 58.9 min.

Methyl 4-((*R*)-hydroxy((*S*)-2-oxocyclohexyl)methyl)benzoate (9e).[38] yield: 15.6 mg, 99%; diastereomer ratio 90:10, determined by ^{1}H NMR of crude product. Colorless solid; mp 62-

64 °C; $[\alpha]^{19}_{D}$ +6.7 (*c* 0.1, $CHCl_3$); ^{1}H NMR (300 MHz, $CDCl_3$) δ 1.16-1.87 (m, 5H), 1.99-2.21 (m, 1H), 2.29-2.69 (m, 3H), 3.92 (s, 1H),4.01 (s, 1H), 4.85 (d, *J* = 8.4 Hz, 1H), 7.40 (d, *J* = 8.4 Hz, 2H), 8.03 (d, *J* = 8.4 Hz, 2H); ^{13}C NMR (75 MHz, $CDCl_3$) δ 24.8, 27.8, 30.8, 42.8, 57.4, 74.4, 121.9, 129.0, 131.7, 140.3, 215.6. Enantiomeric excess of anti-product: 86%, determined by HPLC (Daicel Chiralpak AS-H, Hexane/*i*-PrOH = 80/20), UV λ = 254 nm, flow rate 0.5 mL/min, t_R (2*S*, 1'*R*) 30.3 min , t_R (2*R*,1'*S*) 43.4 min.

(*S*)-2-((*R*)-(4-Methoxyphenyl)(hydroxy)methyl)cyclohexanone (9f).[38] yield: 3.2 mg, 23%; diastereomer ratio 85:15, determined by ^{1}H NMR of crude product. Colorless solid; mp 118-120 °C; $[\alpha]^{19}_{D}$ +13.2 (*c* 0.1, $CHCl_3$); ^{1}H NMR (300 MHz, $CDCl_3$) δ 1.19-1.84 (m, 5H), 2.02-2.13 (m, 1H), 2.29-2.66 (m, 3H), 3.80 (s, 3H), 3.92 (s, 1H), 4.75 (d, *J* = 8.9 Hz, 1H), 6.88 (d, *J* = 8.6 Hz, 2H), 7.24 (d, *J* = 8.6 Hz, 2H); ^{13}C NMR (75 MHz, $CDCl_3$) δ 24.8, 27.9, 30.9, 42.8, 55.4, 57.6, 74.4, 114.0, 128.4, 133.4, 159.5, 216.0. Enantiomeric excess of *anti*-product: 78%, determined by HPLC (Daicel Chiralpak AD-H, Hexane/*i*-PrOH = 90/10), UV λ = 254 nm, flow rate 0.5 mL/min, t_R (2*S*, 1'*R*) 39.7 min , t_R (2*R*,1'*S*) 41.0 min.

(*S*)-2-((*R*)-Hydroxy(phenyl)methyl)cyclohexanone (9g).[38] yield: 8.0 mg, 65%; diastereomer ratio 91:9, determined by ^{1}H NMR of crude product. Colorless solid; mp 99-101 °C; $[\alpha]^{19}_{D}$ +11.7 (*c* 0.1, $CHCl_3$); ^{1}H NMR (300 MHz, $CDCl_3$) δ 1.08-1.90 (m, 5H), 1.98-2.15 (m, 1H), 2.26-2.71 (m, 3H), 3.95 (s, 1H),4.01 (s, 1H), 4.79 (d, *J* = 8.9 Hz, 1H), 7.19-7.70 (m, 5H); ^{13}C NMR (75 MHz, $CDCl_3$) δ 24.8, 27.9, 30.9, 42.8, 57.6, 74.9, 127.3, 128.1, 128.6, 141.2, 215.9. Enantiomeric excess of *anti*-product: 77%, determined by HPLC (Daicel Chiralpak AS-H, Hexane/*i*-PrOH = 90/10), UV λ = 254 nm, flow rate 0.5 mL/min, t_R (2*S*, 1'*R*) 26.0 min, t_R (2*R*,1'*S*) 28.2 min.

(*S*)-2-((*R*)-Hydroxy(4-nitrophenyl)methyl)cyclopentanone (9h).[38] yield: 13.8 mg, 98%; diastereomer ratio 35:65, determined by ^{1}H NMR of crude product. *Anti*-product: colorless solid; mp 87-89 °C; $[\alpha]^{19}_{D}$ -21.3 (*c* 0.1, $CHCl_3$); ^{1}H NMR (300 MHz, $CDCl_3$) δ 1.45-1.85 (m, 3H), 1.95-2.09 (m, 1H), 2.19-2.55 (m, 3H), 4.75 (bs, 1H), 4.85 (d, *J* = 9.1 Hz, 1H)), 7.54 (d, *J* = 8.9 Hz, 2H), 8.22 (d, *J* = 8.9 Hz, 2H); ^{13}C NMR (75 MHz, $CDCl_3$) δ 20.4, 26.9, 38.7, 55.2, 74.6, 123.9, 127.6, 147.9, 148.9, 222.5. Enantiomeric excess of *anti*-product: 78%, determined by HPLC (Daicel Chiralpak AD-H, Hexane/*i*-PrOH = 95/5), UV λ = 254 nm, flow rate 0.5 mL/min, t_R (2*S*, 1'*R*) 90.5 min, t_R (2*R*,1'*S*) 94.3 min.

Residual gold determination

4-Nitrobenzaldehyde (**8a**, 10.0 mg, 0.06 mmol) and GNPs **4c** (6.8 mg, 10 mol% catalyst related to benzaldehyde) or *O*-lauroyl-*trans*-4-hydroxy-l-proline **6** (2.0 mg, 0.006 mmol) were filled in a 2 mL capped glass vial. The cyclohexanone **7a** (69 µL, 0.60 mmol), DMSO/water (94/6) solvent mixture (65 µL) and magnetic stir bar were added to the solid materials and stirred at 25 °C for 24 h. In case of GNP catalyst, the reaction mixture was diluted with EtOAc (1 mL) in order to aggregate GNPs and liquid phase was removed by decantation after 2 min of centrifugation at 4000 rpm. The solid residue was suspended in EtOAc (1 mL) and the previous procedure was used for separation of the liquid phase after 10 min of stirring, and this procedure was repeated twice. The combined organic solution or the reaction mixture (in case of using *O*-lauroyl-*trans*-4-hydroxy-L-proline **6** as a catalyst) was evaporated, solid residue was treated with 0.5 mL aqua regia, diluted with methylene chloride (2 mL) and it was washed with distilled water (10×1.5 mL). The combined water phase was transferred to a volumetric flask and made up to 20.0 mL with distilled water which was used for ICP-OES measurement. For the ICP-OES calibration, 0.001, 0.01, 0.1, 1.0 and 5.0 mg/L gold(III) chloride standard solutions were used and emission intensity measured at 267.595 nm (see Supporting Information).

Monitoring reaction progress of aldol reaction

4-Nitrobenzaldehyde (**8a**, 4.0 mg, 0.03 mmol) and 10 mol% catalyst (**4c**, **5**, **6**; related to **8a**) were added to a NMR tube. Cyclohexanone (**7a**, 27.4 µL, 0.27 mmol) and DMSO-d6/D_2O (94/6) solvent mixture (580 µL) were filled to the solid materials and the reaction mixture was shaked at 25 °C. Conversions were determined by monitoring the reaction mixtures by ^{1}H NMR (see Supporting Information).

■ Acknowledgments

This study was supported in part by a Grant-in-Aid for Young Scientists (A) (No. 23685035) for scientific research from the Japan Society for the Promotion of Science. The authors would like to express their special thanks to Suzuki Motor Corporation for financial support of Péter Lajos Sóti's Fellowship. We also thank Professor N. Sakamoto for the helpful discussion, Mr. S. Takeuchi and Mr. H. Kusanagi for technical support with ICP-OES and elemental analysis measurements.

■ References and Notes

1. MacMillan, D. W. C. *Nature* **2008**, *455*, 304–308.
2. *Stereoselective Organocatalysis: Bond Formation Methodologies and Activation Modes*; Ríos Torres, R., Eds.; John Wiley & Sons, Inc.: Hoboken, New Jersey, 2013.
3. List, B.; Lerner R. A.; Barbas C. F. III *J. Am. Chem. Soc.* **2000**, *122*, 2395–2396.
4. List, B. *J. Am. Chem. Soc.* **2000**, *122*, 9336–9337.
5. List, B.; Pojarlier, P.; Martin, H. J. *Org. Lett.* **2001**, *3*, 2423–2425
6. Ahrendt, K. A.; Borths, C. J.; MacMillan, D. W. C. *J. Am. Chem. Soc.* **2000**, *122*, 4243–4244.
7. List, B. *Tetrahedron* **2002**, *58*, 5573–5587.
8. Itsuno, S.; Haraguchi, N. Supported organocatalysts. In *Science of Synthesis: Asymmetric Organocatalysis*; List, B., Mauroka, K., Eds.; Thieme: Stuttgart, 2012; 673–695.
9. Gruttadauria, M.; Giacalone, F., Noto, R. *Chem. Soc. Rev.* **2008**, *37*, 1666–1688.
10. Ayats, C.; Henseler, A. H.; Pericàs, M. A. *ChemSusChem*. **2012**, *5*, 320–325.
11. Lee, J.-W.; Mayer-Gall, T.; Opwis, K.; Song, C. E.; Gutmann, J. S.; List, B. *Science* **2013**, *341*, 1225–1229.
12. Arakawa, Y.; Wennemers, H. *ChemSusChem*. **2013**, *6*, 242–245.
13. Hernández, J. G.; Juaristi, E. *Chem. Commun* . **2012**, *48*, 5396–5409.
14. Fadhel, A. Z.; Pollet, P.; Liotta, C. L.; Eckert, C. A. *Molecules* **2010**, *15*, 8400–8424.
15. Stevens, P. D.; Fan, J.; Gardimalla, H. M. R.; Yen, M.; Gao Y. *Org. Lett*. **2005**, *7*, 2085–2088.
16. Belser, T.; Stöhr, M.; Pfaltz, A. *J. Am. Chem. Soc.* **2005**, *127*, 8720–8731.
17. Riente, P.; Mendoza, C.; Pericás, M. A. *J. Mater. Chem.* **2011**, *21*, 7350–7355.
18. Wang, B. G.; Ma, B. C.; Wang, Q.; Wang, W. *Adv. Synth. Catal.* **2010**, *352*, 2923–2928.
19. Yacob, Z.; Nan, A.; Liebscher, J. *Adv. Synth. Catal.* **2012**, *354*, 3259–3264.
20. Kong, Y.; Tan, R.; Zhao, L.; Yin, D. *Green Chem.* **2013**, *15*, 2422–2433.
21. Brust, M.; Walker, M.; Bethell, D.; Schiffrin, D. J.; Whyman, R. *J. Chem. Soc., Chem. Commun.* **1994**, 801–802.
22. Brust, M.; Fink, J.; Bethell, D.; Schiffrin, D. J.; Kiely, C. *J. Chem. Soc., Chem. Commun.* **1995**, 1655–1656.
23. Chen, S.; Kimura, K. *Langmuir* **1999**, *15*, 1075-1082.
24. Hostetler, M. J.; Wingate, J. E.; Zhong, C-J.; Harris, J. E.; Vachet, R. W.; Clark, M. R.; Londono, D. J.; Green, J. S.; Stokes, J. J.; Wignall, D. G.; Glish, L. G.; Porter, D. M.; Evans, D. N.; Murray, R. W. *Langmuir* **1998**, *14*, 17–30.

25. Santacruz, L.; Niembro, S.; Santillana, A.; Shafir, A.; Vallri-bera, A. *New J. Chem.* **2014**, *38*, 636–640.
26. Malkov, A. V.; Figlus, M.; Cooke, G.; Caldwell, S. T.; Rabani, G.; Prestly, M. R.; Kočovský, P. *Org. Biomol. Chem.* **2009**, *7*, 1878–1883.
27. Khiar, N.; Navas, R.; Elhalem, E.; Valdivia, V.; Fernández, I. *RSC Advances* **2013**, *3*, 3861–3864.
28. Azcárate, J. C.; Corthey, G.; Pensa, E.; Vericat, C.; Fonticelli, M. H.; Salvarezza, R. C.; Carro, P. J. Phys. *Chem. Lett.* **2013**, *4*, 3127−3138.
29. Corthey, G.; Giovanetti, L. J.; Ramallo-López, J. M.; Zelaya, E.; Rubert, A. A.; Benitez, G. A.; Requejo, F. G.; Fonticelli, M. H.; Sal-varezza, R. C. *ACS Nano* **2010**, *4*, 3413–3421.
30. Naka, K.; Itoh, H.; Chujo, Y. *Bull. Chem. Soc. Jpn.* **2005**, *78*, 501–505.
31. Kristensen, E.T.; Hansen, K. F.; Hansen, T. *Eur. J. Org. Chem.* **2009**, 387–395.
32. Raghuwanshi, V. S.; Ochmann, M.; Hoell, A.; Polzer, F.; Rademann, K. *Langmuir* **2014**, *30*, 6038–6046.
33. For the preparation of **6**, the method of Kristensen *et al.* was used with modifications (see reference 30)
34. Hoang, L.; Bahmanyar, S.; Houk, K. N.; List, B. *J. Am. Chem. Soc.* **2003**, *125*, 16–17.
35. Gruttadauria, M.; Giacalone, F.; Mossuto Marculescu, A.; Lo Meo, P.; Riela, S.; Noto, R. *Eur. J. Org. Chem.* **2007**, 4688–4698.
36. Li, J.; Yang, G.; Qin, Y.; Yang, X.; Cui, Y. *Tetrahedron: Asymmetry* **2011**, *22*, 613–618.
37. Locatelli, E.; Ori, G.; Fournelle, M.; Lemor, R.; Montorsi, M.; Franchini, M. C. *Chem. Eur. J.* **2011**, *17*, 9052–9056.
38. Mase, N.; Nakai, Y.; Ohara, N.; Yoda, H.; Takabe, K.; Tanaka, F.; Barbas, C. F. III *J. Am. Chem. Soc.* **2006**, *128*, 734–735.

■ **Tables**

Table 1. Self-assembly of GNP-supported organocatalysts

entry	cata-lyst	$NaBH_4$	addition time (min)	catalyst loading (mmol g^{-1})[a]	particle size (nm)[b]
1	**4a**	solid	<1	0.50	-
2	**4b**	solution	30	0.71	~3
3	**4c**	solution	60	0.95	~3

[a] Determined by elemental analysis based on the nitrogen atom wt% (nitrogen as an indicator atom for the proline moiety on the Au core). [b] Determined based on TEM analysis.

Table 2. GNP-supported proline-catalyzed asymmetric aldol reactions.

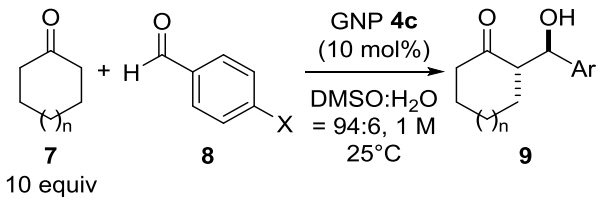

entry	n	X	time (h)	yield (%)[a]	dr[b]	ee (%)[c]	pro-duct
1	1	NO_2	24	97	90:10	88	**9a**
2	1	Cl	72	99	91:9	89	**9b**
3	1	Br	72	90	90:10	87	**9c**
4	1	CN	48	99	90:10	83	**9d**
5	1	CO_2Me	72	99	90:10	86	**9e**
6	1	OMe	166	23[e]	85:15	78	**9f**
7	1	H	120	65	91:9	77	**9g**
8	0	NO_2	5	98	35:65	78	**9h**

[a] Isolated yield. [b] Determined by ^{1}H-NMR (*anti*:*syn*). [c] Enantiomeric excesses of the *anti*-products were determined by chiral HPLC analysis. [e] Conversion of the aldehyde was 31% based on ^{1}H-NMR.

Table 3. Recycling of GNP-supported proline catalyst **4c**

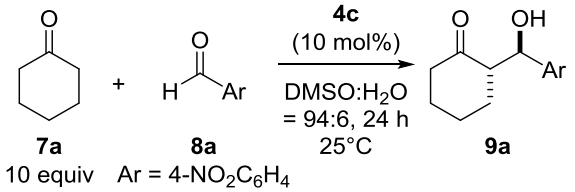

cycles	conversion (%)[a]	yield (%)[b]	dr[c]	ee (%)[d]	recovery
1	98	97	90:10	88	≥99
2	99	98	91:9	88	≥99
3	99	98	91:9	88	≥99
4	99	98	92:8	88	≥99
5	99	98	92:8	88	≥99

[a] Determined by ^{1}H-NMR. [b] Isolated yield. [c] Determined by ^{1}H-NMR (*anti*:*syn*). [d] Enantiomeric excesses of the *anti*-products were determined by chiral HPLC analysis.

Table 4. Comparison of unsupported catalysts (**5** and **6**) and GNP catalyst in the aldol reaction

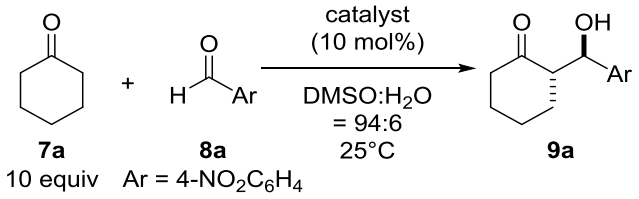

entry	catalyst	concentration (M)	time (h)	yield (%)[a]	dr[b]	ee (%)[c]
1	**5**	1	16	97	86:14	94
2	**6**	1	16	98	92:8	95
3	**4b**	1	24	98	83:17	73
4	**4c**	1	24	97	90:10	88
5[d]	**4c**	1	40	97	94:6	94
6	**5**	0.05	72	97	95:5	74
7	**6**	0.05	72	98	97:3	76
8	**4c**	0.05	90	98	92:8	89

[a] Isolated yield. [b] Determined by ^{1}H-NMR (*anti*:*syn*). [c] Enantiomeric excesses of the *anti*-products were determined by chiral HPLC analysis. [d] The reaction was carried out at 0 °C with 20 mol% catalyst.

■ **Figures**

Graphical Abstract

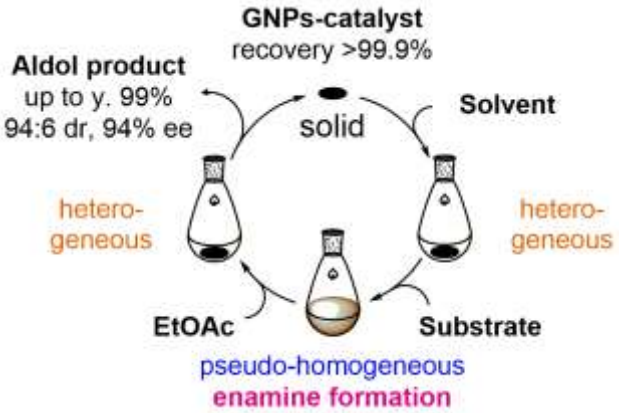

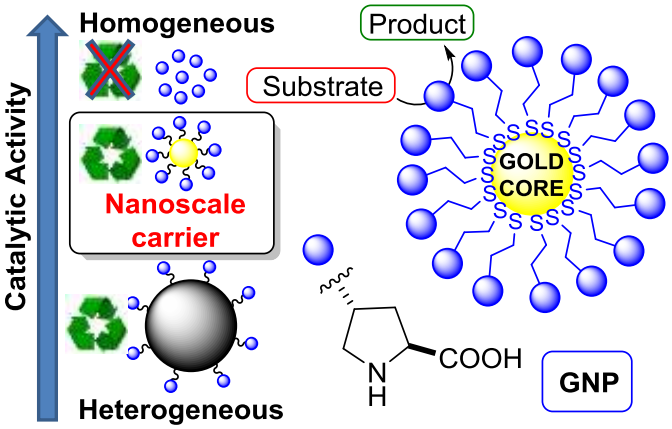

Figure 1. GNP-supported L-proline derivatives as organocatalysts

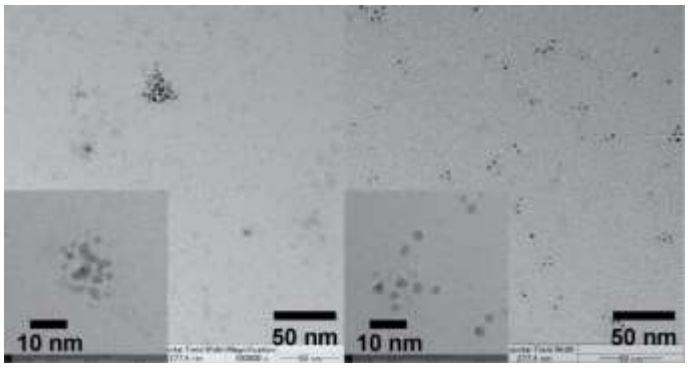

Figure 2. TEM Images of GNPs **4b** (left) and **4c** (right)

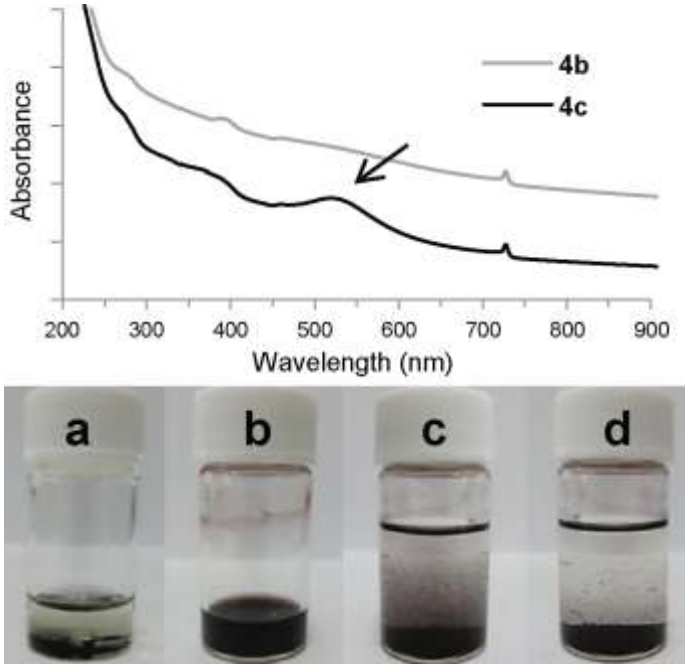

Figure 3. Colloidal behavior of supported catalyst: UV/VIS spectra of **4b** and **4c**; Images of reaction mixtures: (a) at 0 h, (b) after 24 h, (c) after addition of EtOAc and (d) following 2 min of storage.

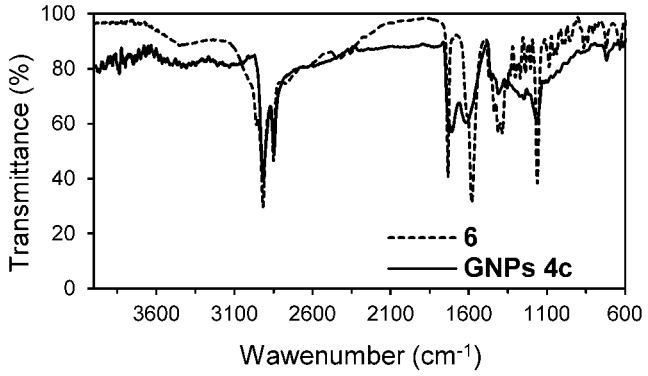

Figure 4. IR spectra of **4c** and **6**

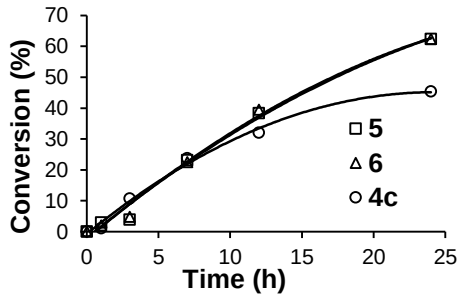

Figure 5. Comparison of unsupported catalysts (**5** and **6**) and GNP catalyst (**4c**) in the aldol reaction. (See the reaction conditions in the Table 4 entry 6, 7, and 8).

■ Schemes

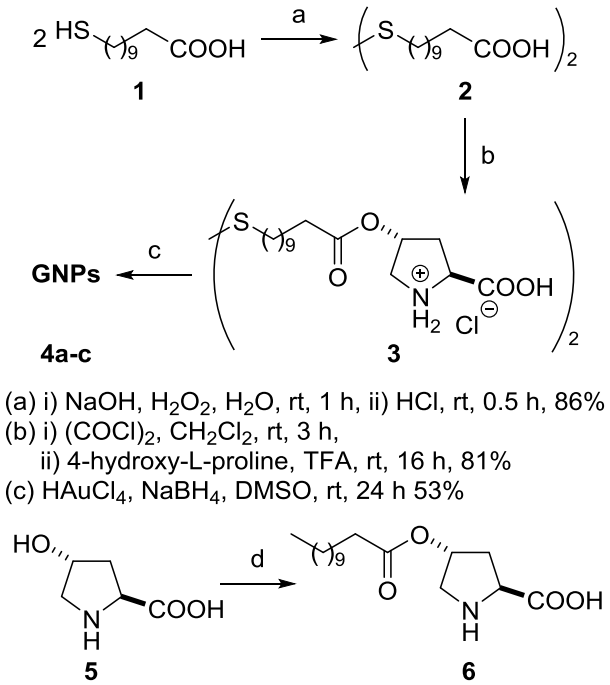

(a) i) NaOH, H_2O_2, H_2O, rt, 1 h, ii) HCl, rt, 0.5 h, 86%
(b) i) $(COCl)_2$, CH_2Cl_2, rt, 3 h,
ii) 4-hydroxy-L-proline, TFA, rt, 16 h, 81%
(c) $HAuCl_4$, $NaBH_4$, DMSO, rt, 24 h 53%

(d) i) lauroyl chloride, TFA, rt, 2 h
ii) K_2CO_3, H_2O, rt, 10 min
iii) AcOH, rt, 10 min, 62%

Scheme 1. Synthesis of GNP-supported and *O*-lauroyl-*trans*-4-hydroxy-L-proline catalysts